

# Melting relations of model lherzolite in the system CaO-MgO-Al<sub>2</sub>O<sub>3</sub>-SiO<sub>2</sub> at 2.4–3.4 GPa and the generation of komatiites

Gudmundur H. Gudfinnsson<sup>1</sup> and Dean C. Presnall

Magmalogy Laboratory, Department of Geosciences, University of Texas at Dallas, Richardson

**Abstract.** Isobarically invariant phase relations in the CaO-MgO-Al<sub>2</sub>O<sub>3</sub>-SiO<sub>2</sub> system (CMAS) involving the lherzolite phase assemblage in equilibrium with liquid have been determined at 2.4–3.4 GPa. These phase relations form the solidus of model lherzolite in the CMAS system. Our data, which include determinations of all phase compositions, are in excellent agreement with the 3.0 and 4.0 GPa points of *Milholland and Presnall* [1991] and *Davis and Schairer* [1965], respectively. The invariant transition on the P-T solidus curve from spinel- to garnet-lherzolite at 3.0 GPa, 1575°C [*Milholland and Presnall*, 1991], is confirmed, but we observe that the theoretically required temperature depression on the solidus curve at this point is not experimentally detectable. Composition trends along the solidus take a sharp turn at the transition. In the spinel-lherzolite stability field, melt compositions become increasingly Fo-normative and less En-normative with increasing pressure, but become less Fo-normative and more pyroxenitic as pressure increases in the garnet-lherzolite stability field. Calculated melting reactions indicate that forsterite is in reaction relationship with the melt up to 3.0 GPa. Orthopyroxene is also in reaction relationship at pressures higher than just over 2.8 GPa and is the only phase in reaction relationship with the melt in the garnet-lherzolite stability field. Comparison of the normative compositions and the CaO/Al<sub>2</sub>O<sub>3</sub> values of the komatiites of Gorgona Island and of the Reliance Formation in Zimbabwe with the compositions of liquids along the solidus of model lherzolite in the CMAS system indicates that the former komatiites were generated at pressures close to 3.7 GPa and the latter at close to 4.5 GPa, assuming that the melt generation occurred in the presence of the complete garnet-lherzolite assemblage.

## Introduction

The system CaO-MgO-Al<sub>2</sub>O<sub>3</sub>-SiO<sub>2</sub> (CMAS) is the simplest chemical system that can have analog phases for all the main lherzolite minerals in equilibrium with melt and, at the same time, constitutes a large part of the chemical composition of the mantle (about 90 wt %). Hence it is the ideal four-component system for investigating phase relations that govern the generation of primary mantle melts.

Other important components are Na<sub>2</sub>O, FeO and, to a lesser extent, TiO<sub>2</sub> and Cr<sub>2</sub>O<sub>3</sub>. *Presnall and Hoover* [1987] and *Walter and Presnall* [1994] studied melting of model lherzolite in the system CMAS + Na<sub>2</sub>O at 0.7–3.5 GPa. They observed that addition of Na<sub>2</sub>O has a strong effect on phase boundaries, resulting in more alkalic primary melts. FeO causes less shift of phase boundaries [*Shi and Libourel*, 1991; *G. H. Gudfinnsson and D. C. Presnall*, manuscript in preparation, 1996]. The volatile components H<sub>2</sub>O and CO<sub>2</sub> can have a very strong effect on the composition of primary basalts [e.g., *Kushiro*, 1972a; *Eggler*, 1978]. However, the source of most mid-ocean ridge basalts, even close to hot spots, appears to contain very small amounts of H<sub>2</sub>O, 450 ppm or less [*Michael*, 1988]. The C content of the upper mantle is estimated to be in the range

50–250 ppm [*Trull et al.*, 1993]. Furthermore, mid-ocean ridge basalts are generated by relatively large aggregate degrees of melting, generally >5% [e.g., *Klein and Langmuir*, 1987; *Johnson et al.*, 1990], which lessens the importance of small amounts of volatiles. Thus volatile-free melting relations are a good approximation for many basalts.

In the CMAS system, forsterite, enstatite, diopside, and one of the aluminous phases, anorthite, spinel, or garnet, coexist with melt at isobaric invariant points, and these isobaric invariant points form the solidus of simplified lherzolite in the CMAS system. At a fixed pressure in the CMAS system, the lherzolite assemblage and melt can exist only at a single temperature, and each of the coexisting phases has a uniquely defined composition, independent of the bulk composition.

*Davis and Schairer* [1965] studied melting relations of the Di-Fo-Py join in the CMAS system at 1 atm and 4.0 GPa. They constrained the composition of the 4.0 GPa garnet-lherzolite invariant point. *Kushiro* [1972b] determined the isobaric invariant point involving the spinel-lherzolite assemblage and melt at 1.0 GPa. *Presnall et al.* [1979] mapped the solidus of simplified lherzolite in the CMAS system from 1 atm to 2.0 GPa. They showed that the transition from plagioclase- to spinel-lherzolite occurs at 0.93 GPa and that this transition creates a cusp on the model lherzolite solidus. They also suggest that a comparable cusp on the solidus of mantle peridotite could cause enhanced melting of upwelling mantle at around 30 km depth. *Milholland and Presnall* [1991] found that the spinel- to garnet-lherzolite transition on the CMAS solidus occurs at 3.0 GPa, 1575°C. At still higher pressures, *Fujii et al.* [1989], using

<sup>1</sup>Now at Centre for Experimental and Theoretical Study of the Earth's Interior, Department of Geology, University of Bristol, Bristol, England.

**Table 1.** Starting Compositions

	CaO	MgO	Al <sub>2</sub> O <sub>3</sub>	SiO <sub>2</sub>
CMAS-6	9.57	28.14	13.56	48.73
CMAS-30	12.75	23.99	16.13	47.13

In weight percent.

a multianvil press, determined the isobaric invariant point at 5.4 GPa. Also, on the basis of multianvil experiments, *Herzberg and Gasparik* [1991] constrained garnet-lherzolite invariant points in the CMAS system from 8.0 to 16.0 GPa. *Herzberg* [1992] wrote equations to describe melt compositions on the solidus of garnet-lherzolite based on these and other experiments. In this paper we present results of melting experiments that constrain the solidus of simplified lherzolite in the CMAS system in the 2.4–3.4 GPa range.

## Experimental and Analytical Procedures

Starting materials were made from mixtures of high-purity oxides and CaCO<sub>3</sub>, which were finely ground and then fired and quenched. The resulting glasses were ground to a powder in an agate mortar. Compositions of starting materials are listed in Table 1. All the experiments were conducted using solid-media piston-cylinder presses [*Boyd and England*, 1960] at the University of Texas at Dallas, using the hot piston-out technique with no pressure correction [*Presnall et al.*, 1978]. The pressure cell assembly is similar to the one described by *Presnall et al.* [1973] with the exception that Pyrex sleeves were used instead of boron nitride and crushable alumina instead of mullite and fired pyrophyllite. To ensure anhydrous experiments, the sample and all the assembly parts, except the Pyrex and talc sleeves, were dried at 1050°C for 1 hour just prior to the start of the runs. Samples were contained in Pt capsules 2.5 mm long and 2.5 mm in diameter. The temperature gradient across the length of the capsule is estimated to be 10°C [*Walter and Presnall*, 1994]. During runs, the temperature was monitored by W5Re/W26Re thermocouples with no pressure correction applied to the emf. Temperature was automatically controlled within ±3°C, and pressure was controlled within ±0.05 GPa. Run conditions are listed in Table 2.

Because no reversal experiments were conducted in this study, equilibrium has not been proven. However, in earlier studies on the solidus of spinel-lherzolite in the CMAS system [*Presnall*, 1976] and on joins in the CMAS system [*Presnall et al.*, 1978; *Sen and Presnall*, 1984; *Liu and Presnall*, 1990], reversal experiments were conducted and attainment of equilibrium in 8 hours or less was demonstrated for the same phases as in this study. The run times of this investigation were 48 hours for the experiments at less than 3.0 GPa and 24 hours for experiments at over 3.0 GPa. On the basis of these earlier studies and the fact that the temperatures in our experiments were higher and thus the reaction rates probably higher, we believe that our experiments represent a close approach to equilibrium. However, some degree of heterogeneity in phase composition, especially in pyroxene compositions, indicates that perfect equilibrium is not reached and, as shown by *Walter and Presnall* [1994], is not likely to be attained in experiments of reasonable length. In experiments of up to 72 hours duration in the CMASN system containing the lherzolite assemblage, *Walter and Presnall* [1994] observed no improvement in pyroxene homogeneity after 48 hours.

Identification and analysis of phases were done with the JEOL 8600 Superprobe at the University of Texas at Dallas. Quantitative analyses were obtained by means of wavelength dispersive spectrometry. A 15-kV accelerating potential was used for all analyses. Pyroxenes, garnet, and olivine were analyzed using a focused beam and a 20-nA beam current; spinel was analyzed using a 5-nA beam current and a focused beam; and glass and quench crystals were analyzed using 10 nA and a 5- to 15-μm beam diameter. Counting time for all elements in all phases was 40 s. Natural and synthetic standards were used. For glass analyses, the phi-rho-Z correction procedure [*Heinrich*, 1986] was applied, but the Bence-Albee procedure [*Albee and Ray*, 1970] was used for all other phases. Compositions of glass, orthopyroxene, clinopyroxene, and garnet are listed in Table 3. Only a few analyses were made of olivine and spinel because these phases are nearly stoichiometric. Olivine is forsterite with about 0.4 wt % CaO and 0.3 wt % Al<sub>2</sub>O<sub>3</sub>, and spinel is nearly pure MgAl<sub>2</sub>O<sub>4</sub> with only 0.1–0.2 wt % CaO and about 0.5 wt % SiO<sub>2</sub>. Some plucking of quench crystals was noticed, and the possibility of preferential removal of one quench phase cannot be entirely discounted, although visual inspection did not show signs of this having occurred.

## Solidus of Model Lherzolite

The model lherzolite solidus in the CMAS system from 1 atm to 4.0 GPa is shown in Figure 1. In addition to our points, we have included 1-atm to 2.0-GPa data from *Presnall et al.* [1979], a 3.0-GPa point from *Milholland and Presnall* [1991], and a 4.0-GPa point from *Davis and Schairer* [1965]. These data are all in excellent agreement with our solidus temperatures and liquid compositions. *Presnall et al.* [1979] found a prominent temperature depression, or a cusp, on the solidus where the transition from plagioclase- to spinel-lherzolite takes place. A cusp is theoretically required [*Schreinemakers*, 1915a, b, c; *Presnall et al.*, 1979] because the solidus above and below the transition is two different univariant lines in P-T space. The univariant lines emanate from the transition, which, accordingly, is an invariant point. The transition on the solidus at 3.0 GPa from spinel- to garnet-lherzolite is an identical occurrence. However, the present data show that at the spinel- to garnet-lherzolite transition, the temperature depression is small and cannot be resolved within the temperature uncertainty of the experiments. Because addition of other components will spread the transition over some pressure interval, the temperature depression on the mantle solidus at the spinel- to garnet-lherzolite transition is probably not discernible. The subsolidus transition is taken from *Gasparik* [1984]. He bracketed the transition up to a

**Table 2.** Run Conditions

Run	Mixture	P, GPa	T, °C	Time, hours	Assemblage <sup>a</sup>
24.30.7	CMAS-30	2.4	1495	48	fo+opx+cpx+sp+gl
26.30.5	CMAS-30	2.6	1525	48	fo+opx+cpx+sp+gl
28.30.2	CMAS-30	2.8	1550	24	fo+opx+cpx+sp+gl
32.6.2	CMAS-6	3.2	1595	24	fo+opx+cpx+gt+gl+qu
33.6.1	CMAS-6	3.3	1605	48	fo+cpx+gt+gl
33.6.2	CMAS-6	3.3	1610	48	fo+opx+gt+(cpx)+qu
34.6.3	CMAS-6	3.4	1615	24	fo+opx+cpx+gt+qu

<sup>a</sup>fo is forsterite, opx is orthopyroxene, cpx is clinopyroxene, sp is spinel, gt is garnet, gl is glass, and qu is quench. Parentheses denote disequilibrium phase.

**Table 3.** Compositions of Run Products

	Run					
	24.30.7	26.30.5	28.30.2	32.6.2	33.6.2	34.6.3
P, GPa	2.4	2.6	2.8	3.2	3.3	3.4
<i>Glass and Quench</i>						
CaO	14.16 (0.02)	14.00 (0.02)	13.67 (0.02)	13.29 (0.08)	13.51 (0.15)	12.70 (0.09)
MgO	19.91 (0.05)	20.46 (0.05)	21.33 (0.04)	22.71 (0.05)	23.32 (0.10)	23.81 (0.08)
Al <sub>2</sub> O <sub>3</sub>	17.62 (0.05)	17.68 (0.05)	17.38 (0.04)	15.96 (0.06)	15.68 (0.08)	14.46 (0.13)
SiO <sub>2</sub>	48.14 (0.03)	47.74 (0.05)	47.25 (0.04)	47.05 (0.10)	48.17 (0.06)	48.18 (0.13)
Total	99.83 (0.10)	99.88 (0.08)	99.63 (0.04)	99.01 (0.07)	100.68 (0.08)	99.15 (0.05)
<i>Orthopyroxene</i>						
CaO	2.65 (0.02)	2.67 (0.02)	2.70 (0.02)	2.77 (0.05)	2.84 (0.02)	2.81 (0.04)
MgO	34.26 (0.08)	34.58 (0.08)	34.15 (0.08)	34.24 (0.11)	34.65 (0.05)	35.21 (0.12)
Al <sub>2</sub> O <sub>3</sub>	8.86 (0.21)	8.97 (0.19)	9.26 (0.26)	8.83 (0.23)	7.98 (0.08)	6.83 (0.25)
SiO <sub>2</sub>	53.94 (0.11)	53.69 (0.10)	53.76 (0.14)	54.07 (0.14)	54.74 (0.07)	55.34 (0.15)
Total	99.71 (0.09)	99.91 (0.07)	99.88 (0.07)	99.91 (0.06)	100.21 (0.08)	100.18 (0.10)
<i>Orthopyroxene: Cations per Six Oxygen Atoms</i>						
Ca	0.096	0.095	0.098	0.100	0.103	0.101
Mg	1.727	1.741	1.719	1.723	1.738	1.767
Al	0.353	0.357	0.369	0.351	0.317	0.271
Si	1.824	1.813	1.815	1.825	1.842	1.863
Total	4.00	4.006	4.000	3.999	3.999	4.002
<i>Clinopyroxene</i>						
CaO	15.03 (0.12)	14.40 (0.09)	13.99 (0.10)	13.02 (0.08)	13.10 (0.09)	13.28 (0.09)
MgO	23.47 (0.13)	24.31 (0.08)	24.47 (0.10)	25.36 (0.14)	25.60 (0.07)	25.90 (0.18)
Al <sub>2</sub> O <sub>3</sub>	10.01 (0.11)	9.94 (0.03)	9.93 (0.07)	9.55 (0.20)	8.80 (0.18)	8.19 (0.30)
SiO <sub>2</sub>	51.11 (0.08)	51.21 (0.06)	51.43 (0.06)	51.84 (0.17)	52.57 (0.13)	52.68 (0.19)
Total	99.62 (0.09)	99.86 (0.08)	99.82 (0.07)	99.77 (0.10)	100.07 (0.08)	100.05 (0.07)
<i>Clinopyroxene: Cations per Six Oxygen Atoms</i>						
Ca	0.565	0.540	0.523	0.486	0.487	0.494
Mg	1.227	1.267	1.273	1.316	1.324	1.342
Al	0.414	0.409	0.409	0.392	0.360	0.336
Si	1.793	1.790	1.795	1.805	1.824	1.830
Total	4.000	4.005	4.000	3.999	3.996	4.002
<i>Garnet</i>						
CaO				5.41 (0.05)	5.23 (0.04)	5.32 (0.10)
MgO				25.14 (0.05)	25.30 (0.04)	25.29 (0.07)
Al <sub>2</sub> O <sub>3</sub>				24.72 (0.03)	24.84 (0.06)	24.82 (0.08)
SiO <sub>2</sub>				44.22 (0.03)	44.49 (0.05)	44.54 (0.05)
Total				99.49 (0.08)	99.86 (0.09)	99.97 (0.13)
<i>Garnet: Cations per 12 Oxygen Atoms</i>						
Ca				0.397	0.381	0.388
Mg				2.564	2.569	2.565
Al				1.993	1.993	1.990
Si				3.024	3.030	3.031
Total				7.977	7.973	7.974

Electron microprobe analyses in weight percent and with standard error of the mean. Ten spots analyzed in each phase, except 20 spots in quench of run 34.6.3.

maximum pressure and temperature of 1400°C, 2.055 GPa, and extrapolated it to the solidus at about 2.2 GPa, in contrast to the solidus intersection at 3.0 GPa later determined by *Milholland and Presnall* [1991]. *Gasparik's* [1984] data can be reconciled with our data and that of *Milholland and Presnall* [1991] only if the transition line has stronger curvature than that shown by *Gasparik*. This stronger curvature (Figure 1) does not violate *Gasparik's* experimental brackets.

Figures 2 and 3 are CIPW molecular normative diagrams that show the trace of the lherzolite isobaric invariant point in the CMAS system from 1 atm to 4.0 GPa. In other words, they show how liquid compositions on the solidus of model lherzolite change with pressure. The good agreement with the 4.0-GPa point of *Davis and Schairer* [1965] is obvious. A recently determined 5.0-GPa point [*Weng and Presnall*, 1995] is also

consistent with the trend defined by our data and the data of *Davis and Schairer* [1965]. It can be seen that primary melts of model lherzolite at low pressure are Q normative, but above ~0.9 GPa they become increasingly Fo normative and move toward the alkalic side of the phase diagram. At 3.0 GPa, however, the trend takes a sharp turn as the melt compositions move away from the alkalic side but also becomes less picritic and more pyroxenitic as pressure increases in the garnet-lherzolite stability field. The variation of each oxide with pressure is shown in Figures 4, 5, 6 and 7. The lines are "cycball" fits, adopted to show the general trends of the data. Theoretically, discontinuities in the slopes of the oxide trends should exist at the spinel- to garnet-lherzolite transition. This is clearly observed for Al<sub>2</sub>O<sub>3</sub> and especially SiO<sub>2</sub>, whereas the change in the MgO and CaO trends is less pronounced. It can be seen that the SiO<sub>2</sub> and MgO con-

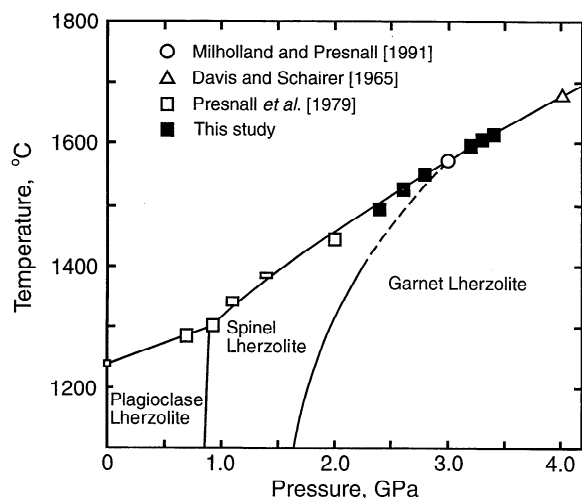


**Figure 1.** Pressure-temperature diagram for the univariant solidus and subsolidus transitions of model lherzolite in the CMAS system from 1 atm to 4.0 GPa. The plagioclase- to spinel-lherzolite subsolidus transition curve is from Presnall *et al.* [1979] and the spinel- to garnet-lherzolite subsolidus transition curve is from Gasparik [1984]. The sizes of the symbols correspond to the estimated uncertainty.

tents of lherzolite melts actually increase simultaneously with pressure in the 3.0–4.0 GPa range.

In Figures 8 and 9 the equation of Herzberg [1992] is used to calculate melt compositions on the garnet-lherzolite solidus in the CMAS system at several different pressures. Also, we include the 5.4-GPa point of Fujii *et al.* [1989] derived from a multianvil experiment. There is clearly a discrepancy between our data and the data of Davis and Schairer [1965] on the one hand and the calculation of Herzberg [1992] and the single point of Fujii *et al.* [1989] on the other. According to our data, the calculated compositions of Herzberg [1992] are consistently too high in MgO. The source of the discrepancy with Fujii *et al.* [1989] is unknown. The discrepancy with Herzberg [1992] could

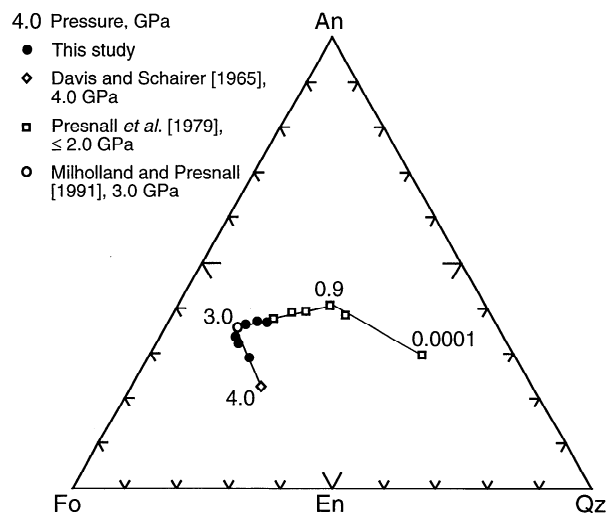


**Figure 2.** Normative diagram showing compositions of liquids along the solidus of model plagioclase-lherzolite (0.0001–0.9 GPa), spinel-lherzolite (0.9–3.0 GPa), and garnet-lherzolite (>3.0 GPa) in the CMAS system from 1 atm to 4.0 GPa. Molecular norm. Projection from Di.

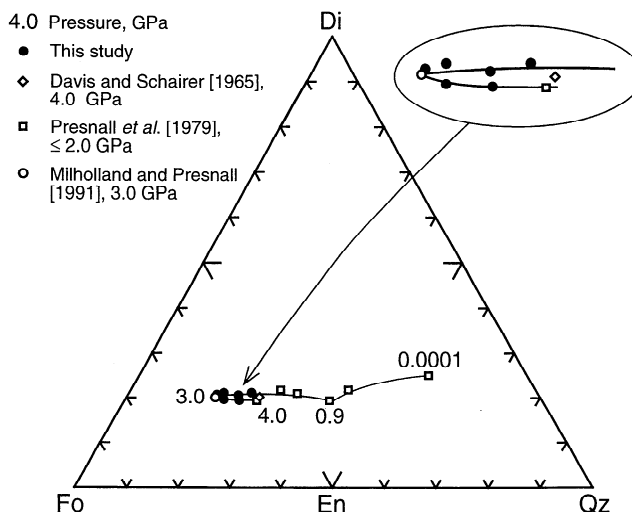


**Figure 3.** Same as Figure 2. Projection from An.

be explained by the fact that he favored the data point of Fujii *et al.* [1989] and assumed that the spinel- to garnet-lherzolite transition at the solidus occurs at 2.2 GPa.

The pyroxenes coexisting along the solidus are ternary solid solutions containing En, Di and Tschermak (Ts) components. There is very little change in the amount of the Ts component of the pyroxenes in the spinel-lherzolite field, and clinopyroxene is slightly higher in Ts component than orthopyroxene (Figure 10). As observed also at lower pressures, the solubility of En in clinopyroxene at the solidus increases steadily with pressure in the spinel-lherzolite stability field. On the basis of an extrapolation of subsolidus pyroxene compositions to the CMAS solidus, Gasparik [1984] assumed that the spinel- to garnet-lherzolite transition intersects the solidus at 2.2 GPa. If his data from the spinel-lherzolite stability field are extrapolated to 3.0 GPa, they seem to be in good agreement with our determined compositions, although our data indicate some-

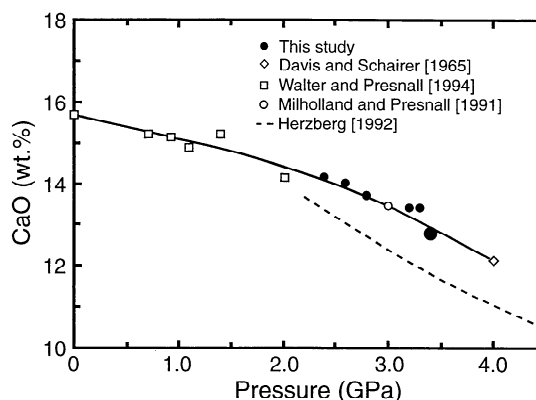


**Figure 4.** Diagram depicting the variation of CaO in melts along the solidus of model lherzolite in the CMAS system as a function of pressure. The 1-atm to 1.4-GPa points are from Presnall *et al.* [1979], as reanalyzed by Walter and Presnall [1994]. The 2.0-GPa point is an unpublished run by J. D. Hoover, analyzed and reported by Walter and Presnall [1994]. The dashed line is a calculated trend from the equation for melt compositions along the solidus of garnet-lherzolite in the CMAS system given by Herzberg [1992]. The standard errors of the analyses in this study are smaller than the symbols.

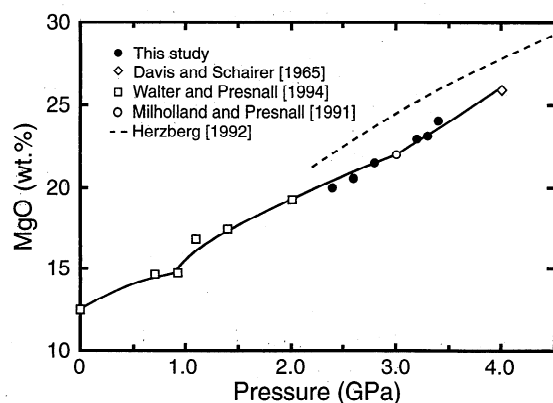
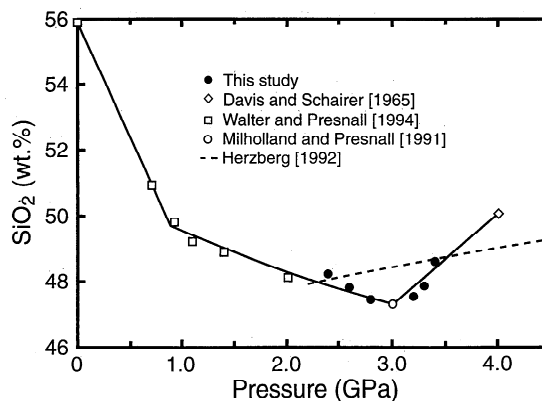


Figure 5. Same as Figure 4 for MgO.

Figure 7. Same as Figure 4 for SiO<sub>2</sub>.

what larger amounts of Ca-Ts component in clinopyroxene than he estimated (Figure 10). As predicted by *Gasparik* [1984], the amount of *Ts* component in both pyroxenes decreases sharply with increasing pressure in the garnet field. The composition of garnet on the solidus just above the spinel/garnet transition is a pyrope-grossular solid solution close to Py<sub>87</sub>-Gr<sub>13</sub>.

### Melting Reactions

In isobarically invariant equilibria, the proportions of the coexisting phases can only change according to uniquely defined chemical reactions. *Korzhinskii* [1959] showed that if the composition of all the coexisting phases is known, such a reaction can be balanced by means of determinants [Presnall, 1986]. Melting reactions along the solidus of model lherzolite in the CMAS system calculated by *Korzhinskii's* [1959] method are shown in Table 4. Because the reaction coefficients change continuously with pressure, they are listed at several different pressures. The reaction is always of the peritectic type. Up to a pressure somewhere between 2.8 and 3.0 GPa, forsterite is the only phase in reaction relationship with the melt. A singular point occurs between 2.8 and 3.0 GPa, above which forsterite is joined by orthopyroxene in reaction relationship, but above the transition at 3.0 GPa from spinel- to garnet-lherzolite, orthopyroxene is the sole phase in reaction relationship with the melt.

Melting continues according to these reactions as long as all

the lherzolite phases are present. The bulk composition of the lherzolite determines which phase is first eliminated and how much melting occurs before that happens. When the first phase is eliminated, the melting reaction changes and as temperature rises the reaction coefficients change continuously. The melting reaction also depends on the bulk composition when the system has higher variance than that of the isobaric invariant points. This would be the case for natural lherzolites, which are strictly multivariant systems. In the system CaO-MgO-Al<sub>2</sub>O<sub>3</sub>-SiO<sub>2</sub>-Na<sub>2</sub>O (CMASN), model lherzolite melts along isobaric univariant lines. The CMASN melting reactions presented by *Walter et al.* [1995] compare favorably with melting reactions of model lherzolite in the CMAS system, especially when evaluated over a large melting interval (Table 5). Both sets of reactions broadly agree on the relative proportions of phases in the reactions and the way in which the proportions change with pressure. In the CMASN system, orthopyroxene is in reaction relationship on the solidus down to about 2.0 GPa, but if melting is assessed over a larger melting interval, only forster-

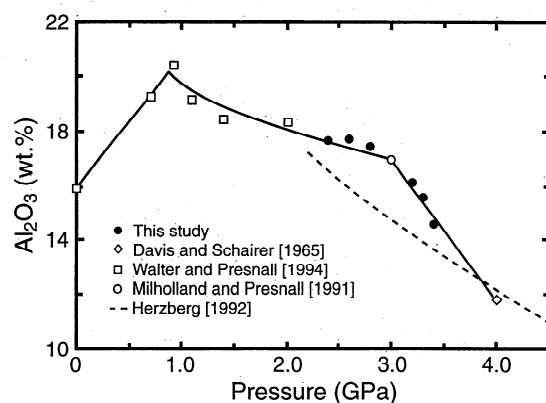
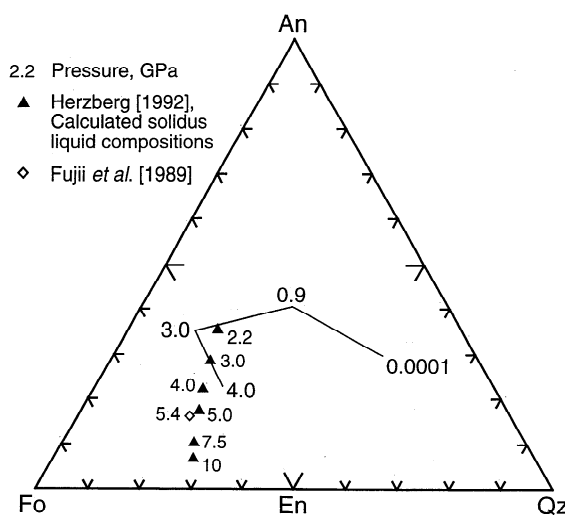
Figure 6. Same as Figure 4 for Al<sub>2</sub>O<sub>3</sub>.

Figure 8. Normative diagram comparing the compositions of liquids along the solidus of model lherzolite in the CMAS system (Figure 2) with calculated compositions of liquids on the solidus of garnet-lherzolite in the CMAS system from the equation of *Herzberg* [1992]. Also shown is a 5.4-GPa point from *Fujii et al.* [1989]. Molecular norm. Projection from Di.

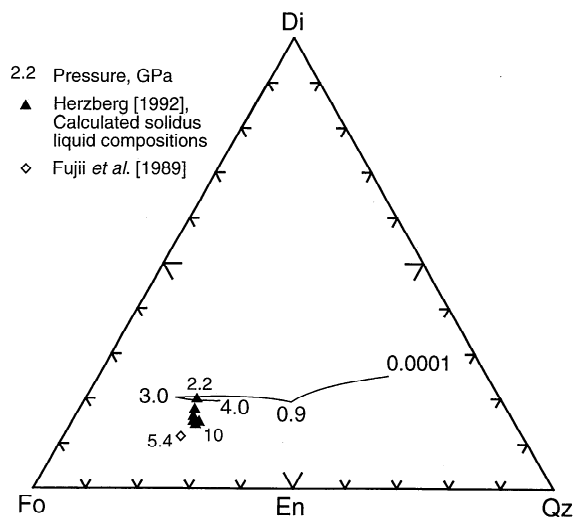


Figure 9. Same as Figure 8. Projection from An.

ite is in reaction relationship at that pressure, as is the case on the CMAS solidus.

Walter *et al.* [1995] showed that for large melting intervals where comparisons are valid, melting reactions in the CMASN system are in close agreement with reactions calculated from experiments on natural basalts. The similarity, in turn, of melting reactions in the CMAS and CMASN systems shows that inclusion of additional components beyond CMAS provides only modest improvement in the coefficients for the melting reactions. This reinforces the conclusion of Walter *et al.* [1995] that melting reactions in the CMASN system can be confidently used for quantitative trace element modeling of natural compositions.

## Generation of Komatiites

Komatiites are high-MgO lavas that could in some cases represent near-primary high-pressure melts. Most examples of komatiites are from the Archean. They are ultramafic volcanic

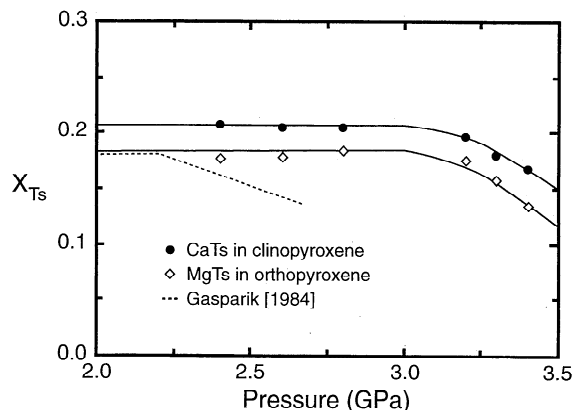


Figure 10. Variation diagram depicting the mole fraction of Ca-Tschermak component in clinopyroxene and Mg-Tschermak component in orthopyroxene on the CMAS solidus as a function of pressure. Shown for comparison are similar data of Gasparik [1984] which he derived by extrapolation to the solidus. The Tschermak components in Gasparik's [1984] solidus clinopyroxene and orthopyroxene are very similar and have therefore been shown as one line.

rocks and among their diagnostic features is spinifex texture [Arndt and Nisbet, 1982], which suggests their origin as liquids. In addition to high MgO contents, some other aspects of their chemistry are unusual for volcanic rocks, such as their high CaO/Al<sub>2</sub>O<sub>3</sub> value. Komatiites also tend to have low concentrations of incompatible elements, which has been attributed to relatively large degrees of melting, in some cases far over 50 wt % [e.g., Nesbitt and Sun, 1976]. Campbell *et al.* [1989] proposed that komatiites are products of melting in abnormally hot mantle jets, which were perhaps the Archean equivalent of present-day mantle plumes. This proposal is supported by the large difference between the eruption temperature of komatiites, estimated from their MgO contents, and the average potential mantle temperatures in the Archean, predicted by secular cooling models for the mantle [Nisbet *et al.*, 1993]. Also, an ion microprobe study of komatiites from the Reliance Formation [McDonough and Ireland, 1993] indicates that the ratios of mobile to immobile incompatible elements in glass inclusions in olivines in these rocks are similar to those of modern intraplate basalts and differ from those found in modern mid-ocean ridge and convergent margin basalts. Although most workers have postulated that komatiite magmas had unusually high temperatures, this contention is not without controversy. Grove *et al.* [1994] argued, on the basis of textural evidence, that the 3.49 Ga Barberton Mountainland komatiites were wet and that their eruption temperature was only about 1200°C.

Because of their considerable age, most komatiites are highly altered, and in many cases none of the primary minerals and glasses have survived. This makes determinations of primary mineralogy and original chemical composition highly uncertain. Nisbet *et al.* [1993] disputed early estimates of over 30 wt % MgO for komatiite liquids as they may have contained olivine phenocrysts, and they argued that the highest known MgO content of a komatiite melt is probably less than this amount. All komatiites have been altered to some degree [Nisbet *et al.*, 1993], but one way around the problem with the interpretation of the primary composition is to use only the freshest samples. Figures 11 and 12 show normative compositions of komatiites from the Reliance Formation in the Belingwe greenstone belt [Nisbet *et al.*, 1987] and from Gorgona Island [Aitken and Echeverría, 1984]. Although komatiites of the Reliance Formation are about 2.7 Ga old, they are remarkably fresh for their age and even contain some pristine olivine. The Gorgona Island komatiites are younger than other known komatiites, being Mesozoic in age, and are relatively fresh. Renner *et al.* [1994] pointed out the problems of determining the composition of erupted komatiite liquids, even in the case of well-preserved komatiites, because of the extensive differ-

Table 4. Melting Reactions

P, GPa	Melting Reaction, wt %
0.0001 <sup>a</sup>	49 opx + 20 cpx + 31 an = 79 liq + 21 fo
0.7	32 opx + 27 cpx + 41 an = 93 liq + 7 fo
1.1	36 opx + 55 cpx + 9 sp = 77 liq + 23 fo
2.0 <sup>b</sup>	23 opx + 68 cpx + 9 sp = 84 liq + 16 fo
2.4	14 opx + 78 cpx + 8 sp = 85 liq + 15 fo
2.8	4 opx + 87 cpx + 9 sp = 89 liq + 11 fo
3.4	2 fo + 68 cpx + 30 gt = 78 liq + 22 opx

<sup>a</sup>The 0.0001, 0.7, and 1.1 GPa experiments are from Presnall *et al.* [1979] and reanalyzed by Walter and Presnall [1994].

<sup>b</sup>Unpublished experiment by J. D. Hoover, reanalyzed by Walter and Presnall [1994].

**Table 5.** Comparison of Melting Reactions in the CMAS and CMASN Systems

System	P, GPa	Melting Interval	Melting Reaction, wt %
CMAS	0.7	invariant	32 opx + 27 cpx + 41 an = 93 liq + 7 fo
CMASN <sup>a</sup>	0.7	solidus	24 opx + 26 cpx + 50 pl = 95 liq + 5 fo
CMASN	1.0	10–22%	34 opx + 56 cpx + 10 sp = 75 liq + 25 fo
CMAS	1.1	invariant	36 opx + 55 cpx + 9 sp = 77 liq + 23 fo
CMAS	2.0	invariant	23 opx + 68 cpx + 9 sp = 84 liq + 16 fo
CMASN	2.0	0–<1%	91 cpx + 9 sp = 72 liq + 9 fo + 19 opx
CMASN	2.0	0–10%	89 cpx + 11 sp = 85 liq + 12 fo + 3 opx
CMAS	3.4	invariant	2 fo + 68 cpx + 30 gt = 78 liq + 22 opx
CMASN	3.5	solidus	6 fo + 71 cpx + 23 gt = 52 liq + 48 opx

<sup>a</sup>From *Walter et al.* [1995]. Calculated by the mass proportion method using composition model lherzolite A.

entiation that took place after they erupted. Therefore we have opted to plot series of whole rock analyses. Both in the case of the Gorgona komatiites [*Aitken and Echeverría*, 1984] and the Reliance komatiites [*Renner et al.*, 1994], olivine is believed to be the main fractionating phase, and this is manifested on Figures 11 and 12 by the samples lining up close to olivine fractionation lines. The MgO content of the depicted komatiites of the Reliance Formation varies from 15 to 27 wt %, whereas the range is 13–24 wt % for Gorgona Island. *Aitken and Echeverría* [1984] calculated the composition of the fractionating olivine in the Gorgona Island komatiites as Fo<sub>90.5</sub> and then used the Fe-Mg exchange coefficient between olivine and liquid of 0.33 to estimate the MgO content of the erupted liquid as 20 wt %. If an exchange coefficient of 0.30 is assumed, then the MgO content changes to about 18 wt % [*Nisbet et al.*, 1993]. In the Reliance Formation the MgO content of the erupted liquid of the lava flow depicted has been estimated as 20 wt % [*Nisbet et al.*, 1993]. If this is correct, some of the rock compositions contain excess olivine, while others are depleted in olivine relative to the primary liquid composition.

On the assumption that the komatiites from Gorgona Island

and the Reliance Formation were generated in equilibrium with olivine, enstatite, diopside, and garnet, our CMAS data together with information on the additional effects of Na<sub>2</sub>O and FeO can be used to estimate depths of origin. We first evaluate depths of origin on this assumption. Then we consider the effects of deviations from this assumption. In Figures 11 and 12 the komatiites plot slightly away from the CMAS solidus, but this can be explained by the absence of FeO and Na<sub>2</sub>O from the CMAS system. The effect of the addition of Na<sub>2</sub>O to the CMAS system is to shift the solidus of model lherzolite toward the alkalic side of the basalt tetrahedron [*Walter and Presnall*, 1994]. The Reliance Formation samples contain about 1 wt % Na<sub>2</sub>O, and the Gorgona Island samples contain 0.6–1.2 wt %. Even these small amounts can have significant effect. Data from the spinel-lherzolite stability field of the CMAS + FeO system indicate that addition of FeO has a smaller effect than addition of Na<sub>2</sub>O (G. H. Gudfinnsson and D. C. Presnall, manuscript in preparation, 1996), but these komatiites contain considerable amounts of FeO (about 10 wt %). Judging from the CMASF data, FeO would cause the phase relations to shift more toward the olivine apex, but we caution that the trends may be somewhat different in the garnet-lherzolite stability field. Considering this, we suggest that the Gorgona Island komatiites could be generated by melting in the 3.0–4.0 GPa range, and the Reliance Formation kom-

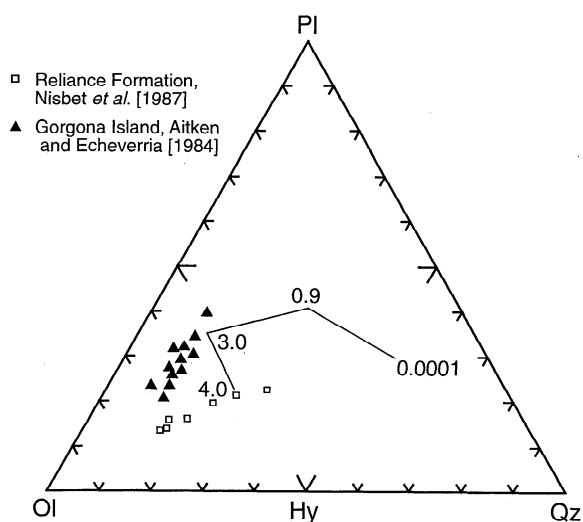


**Figure 11.** Normative diagram comparing the whole rock compositions of komatiites with liquid compositions along the solidus of model lherzolite in the CMAS system. The komatiites are from the Reliance Formation in the Belingwe greenstone belt, Zimbabwe, and Gorgona Island, Colombia.  $\text{Fe}^{2+}/\text{Fe}^{2+} + \text{Fe}^{3+}$  has been set as 0.9. Molecular norm. Projection from Cpx.

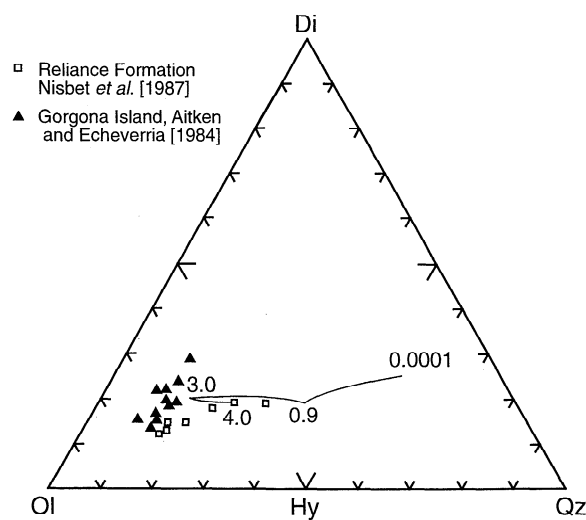


**Figure 12.** Same as Figure 10. Projection from Pl.

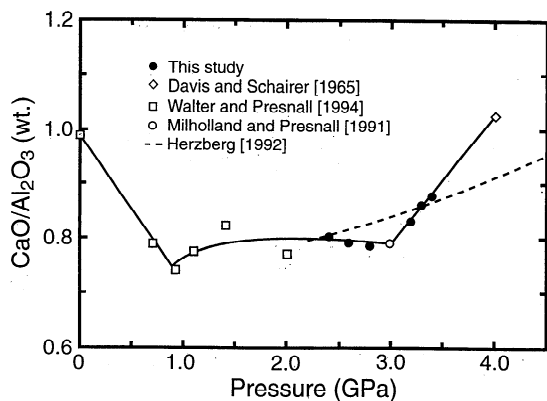


Figure 13. Same as Figure 4 for  $\text{CaO}/\text{Al}_2\text{O}_3$ .

atiites could be generated at somewhat higher pressure, probably in the 4.0–5.0 GPa range.

Herzberg [1992] noted that the  $\text{CaO}/\text{Al}_2\text{O}_3$  value of melts along the solidus of simplified garnet-lherzolite in the CMAS system increases steadily with increasing pressure. He proposed that the  $\text{CaO}/\text{Al}_2\text{O}_3$  value of komatiites could be used to decipher their depth of origin. Figure 13 compares the  $\text{CaO}/\text{Al}_2\text{O}_3$  values of our experimental melts and those of melt compositions calculated by the equation of Herzberg [1992]. The  $\text{CaO}/\text{Al}_2\text{O}_3$  values of our melts increase more strongly with pressure and are in good agreement with the 5.0 GPa experiment of Weng and Presnall [1995] ( $\text{CaO}/\text{Al}_2\text{O}_3 = 1.2$ ). Herzberg [1992] argues that addition of FeO and  $\text{Na}_2\text{O}$  have very little effect on the  $\text{CaO}/\text{Al}_2\text{O}_3$ . The data of G. H. Gudfinnsson and D. C. Presnall (manuscript in preparation, 1996) from the spinel and plagioclase fields indicate that this is correct in the case of FeO, but the data of Walter and Presnall [1994] indicate that  $\text{Na}_2\text{O}$  lowers the  $\text{CaO}/\text{Al}_2\text{O}_3$  value such that if a komatiite primary liquid contains about 1 wt %  $\text{Na}_2\text{O}$ , using Figure 13 to estimate the pressure would cause an underestimation of about 0.5 GPa. Taking this into account and the fact that  $\text{CaO}/\text{Al}_2\text{O}_3$  of the Gorgona Island komatiites is about 0.85 and that of the komatiites of the Reliance Formation is about 1.02, we propose, on the basis of Figure 13, that the former komatiites were generated at around 3.7 GPa and the latter around 4.5 GPa. In the case of the Gorgona Island komatiites, our estimation is close to the estimation of Herzberg [1992], but in the case of the komatiites of the Reliance Formation our estimation is slightly lower. However, these pressure estimations are much lower than those of Nisbet *et al.* [1993] (4.5 and 12 GPa, respectively) based on temperatures derived from MgO contents and olivine compositions.

At pressures above ~4–5 GPa, enstatite disappears from the solidus of mantle peridotite but is produced on melting at temperatures above the solidus for pressures at least up to 7 GPa [Canil, 1992; Zhang and Herzberg, 1994; Walter, 1995]. Therefore small amounts of melting at temperatures very close to the solidus would occur in the absence of enstatite, but for larger amounts of melting at higher temperatures, melting would occur in the presence of the complete garnet-lherzolite assemblage of olivine, enstatite, diopside, and garnet. Thus, for komatiites produced by a very small amount of melting near the solidus at pressures >4 GPa, our depth estimates are not applicable. However, if komatiites are generated by larger degrees of melting, enstatite starts to form, the melt is in equilibrium with the complete garnet-lherzolite assemblage, and

our depth estimates are relevant. A more quantitative discussion of the amount of melting required for these changes to occur as a function of pressure must await more detailed experimental data. Also, at the present state of knowledge, it is not possible to determine with certainty the phases in equilibrium with primary komatiitic liquids at their source, so our depth estimates should be used cautiously.

The discussion above does not consider the possibility of polybaric or near-fractional melting. Geochemical evidence indicates that melting to generate mid-ocean ridge basalts is polybaric, starts in the garnet-lherzolite stability field, and is near-fractional [Salters and Hart, 1989; Johnson *et al.*, 1990], which suggests that if komatiitic melts were formed by mantle upwelling they were also formed by a similar process. As pressure increases, the density difference between residual mantle phases and melt decreases; hence high-pressure melts probably do not segregate as readily from the residue as do lower pressure melts [Stolper *et al.*, 1981]. Consequently, somewhat larger melt fractions may have resided with the residue for komatiite generation than for mid-ocean ridge basalt generation. Nevertheless, melting probably occurred over some pressure range and in this scheme komatiite lavas would represent mixtures of melts and the pressures derived from komatiite compositions would represent average pressures of generation.

## Conclusions

The data presented here on the solidus of simplified lherzolite in the CMAS system at 2.4 to 3.4 GPa are in excellent agreement with the lower pressure data of Presnall *et al.* [1979], the 3.0 GPa data of Milholland and Presnall [1991], and the 4.0 GPa data of Davis and Schairer [1965]. They confirm the previously postulated spinel- to garnet-lherzolite transition on the solidus at 3.0 GPa, 1575°C [Milholland and Presnall, 1991]. Unlike the plagioclase- to spinel-lherzolite transition, there is only a very small solidus cusp at this transition.

The data show that the compositional trend with pressure takes a sharp turn at the spinel- to garnet-lherzolite transition. With increasing pressure in the garnet field the amounts of  $\text{SiO}_2$  and MgO increase at the same time, leading to less picritic and more pyroxenitic melts, whereas in the spinel field the trend is toward steadily more picritic compositions with increasing pressure. The compositional trend in the garnet field is at a high angle to the trend of calculated compositions of Herzberg [1992] and indicates that Herzberg's [1992] compositions are consistently too high in normative Fo.

Melting reactions on the solidus in the range of the experimental data are always of the peritectic type, with forsterite alone in reaction relationship with the melt up to a pressure just over 2.8 GPa where it is joined by orthopyroxene. In the garnet field, orthopyroxene is the only phase that crystallizes on melting on the solidus.

By assuming melt generation in the presence of the complete garnet-lherzolite phase assemblage and by comparing the CMAS solidus compositions and compositions of komatiites from Gorgona Island and the Reliance Formation, we find that they could be generated at around 3.7 and 4.5 GPa pressure, respectively. In the latter case our pressure estimation is slightly lower than that of Herzberg [1992] and much lower than that of Nisbet *et al.* [1993].

**Acknowledgments.** We wish to thank Dave Walker, Tim Grove, Steve Parman, and an anonymous reviewer for useful comments. This



research was supported by National Science Foundation grants EAR-9219159 and EAR-8816044 and by Texas Advanced Research Program grants 009741-044 and 009741-066. While at the University of Bristol, G.H.G. did part of the manuscript preparation and was supported by a NERC grant GR3/10120 to B. J. Wood. Department of Geosciences, University of Texas at Dallas, contribution 843.

## References

- Aitken, B. G., and L. M. Echeverría, Petrology and geochemistry of komatiites and tholeiites from Gorgona Island, Colombia, *Contrib. Mineral. Petrol.*, **86**, 94–105, 1984.
- Albee, A. L., and L. Ray, Correction factors for electron-probe microanalysis of silicates, oxides, carbonates, and sulphates, *Anal. Chem.*, **42**, 1408–1414, 1970.
- Arndt, N. T., and E. G. Nisbet, What is a komatiite?, in *Komatiites*, edited by N. T. Arndt and E. G. Nisbet, pp. 19–27, George Allen Unwin, Winchester, Mass., 1982.
- Boyd, F. R., and J. L. England, Apparatus for phase-equilibrium measurements at pressures up to 50 kilobars and temperatures up to 1750°C, *J. Geophys. Res.*, **65**, 741–748, 1960.
- Campbell, I. H., R. W. Griffiths, and R. I. Hill, Melting in an Archean mantle plume: Head it's basalts, tails it's komatiites, *Nature*, **339**, 697–699, 1989.
- Canil, D., Orthopyroxene stability along the peridotite solidus and the origin of cratonic lithosphere beneath southern Africa, *Earth Planet. Sci. Lett.*, **111**, 83–95, 1992.
- Davis, B. C. T., and J. F. Schairer, Melting relations in the join diopside-forsterite-pyroxene at 40 kilobars and at one atmosphere, *Year Book Carnegie Inst. Washington*, **64**, 123–126, 1965.
- Eggler, D. H., The effect of CO<sub>2</sub> upon partial melting of peridotite in the system Na<sub>2</sub>O-CaO-Al<sub>2</sub>O<sub>3</sub>-MgO-SiO<sub>2</sub>-CO<sub>2</sub> to 35 kb, with an analysis of melting in the peridotite-H<sub>2</sub>O-CO<sub>2</sub> system, *Am. J. Sci.*, **278**, 305–343, 1978.
- Fujii, T., M. Tachikara, and K. Kurita, Melting experiments in the system CaO-MgO-Al<sub>2</sub>O<sub>3</sub>-SiO<sub>2</sub> to 8 GPa: Constraints on the origin of komatiites, *Eos Trans. AGU*, **70**, 483, 1989.
- Gasparik, T., Two-pyroxene thermobarometry with new experimental data in the system CaO-MgO-Al<sub>2</sub>O<sub>3</sub>-SiO<sub>2</sub>, *Contrib. Mineral. Petrol.*, **87**, 87–97, 1984.
- Grove, T. L., G. A. Gaetani, and M. J. de Wit, Spinifex textures in 3.49 Barberton Mountain Belt komatiites: Evidence for crystallization of water-bearing, cool magmas in the Archean, *Eos Trans. AGU*, **75**(16), Spring Meet. Suppl., 354, 1994.
- Heinrich, K. F. J., Comparison of algorithms for X-ray mass absorption coefficients, *Microbeam Analysis*, **21**, 279–280, 1986.
- Herzberg, C., Depth and degree of melting of komatiites, *J. Geophys. Res.*, **97**, 4521–4540, 1992.
- Herzberg, C., and T. Gasparik, Garnet and pyroxenes in the mantle: A test of the majorite fractionation hypothesis, *J. Geophys. Res.*, **96**, 16,263–16,274, 1991.
- Johnson, K. T. M., H. J. B. Dick, and N. Shimizu, Melting in the oceanic upper mantle: An ion microprobe study of diopsides in abyssal peridotites, *J. Geophys. Res.*, **95**, 2661–2678, 1990.
- Klein, E. M., and C. H. Langmuir, Global correlations of ocean ridge basalt chemistry with axial depth and crustal thickness, *J. Geophys. Res.*, **92**, 8089–8115, 1987.
- Korzhinskii, D. S., *Physicochemical Basis of the Analysis of the Paragenesis of Minerals*, Consultants Bureau, New York, 1959.
- Kushiro, I., Effect of water on the composition of magmas formed at high pressures, *J. Petrol.*, **13**, 311–334, 1972a.
- Kushiro, I., Partial melting of synthetic and natural peridotites at high pressures, *Year Book Carnegie Inst. Washington*, **71**, 357–362, 1972b.
- Liu, T.-C., and D. C. Presnall, Liquidus phase relationships on the join anorthite-forsterite-quartz at 20 kbar with applications to basalt petrogenesis and igneous sapphirine, *Contrib. Mineral. Petrol.*, **104**, 735–742, 1990.
- McDonough, W. F., and T. R. Ireland, Intraplate origin of komatiites inferred from trace elements in glass inclusions, *Nature*, **365**, 432–434, 1993.
- Michael, P. J., The concentration, behavior and storage of H<sub>2</sub>O in the suboceanic upper mantle: Implications for mantle metasomatism, *Geochim. Cosmochim. Acta*, **52**, 555–566, 1988.
- Milholland, C. S., and D. C. Presnall, Is the aluminous pyroxene plane a thermal divide at high pressures? Evidence from liquidus phase relationships in the system CaO-MgO-Al<sub>2</sub>O<sub>3</sub>-SiO<sub>2</sub> at 30 kbar, *Eos Trans. AGU*, **72**(44), Fall Meet. Suppl., 548, 1991.
- Nesbitt, R. W., and S.-S. Sun, Geochemistry of Archean spinifex textured peridotites and magnesian and low magnesian tholeiites, *Earth Planet. Sci. Lett.*, **31**, 433–453, 1976.
- Nisbet, E. G., N. T. Arndt, M. J. Bickle, W. E. Cameron, C. Chauvel, M. Cheadle, E. Hegner, T. K. Kyser, A. Martin, R. Renner, and E. Roedder, Uniquely fresh 2.7 Ga komatiites from the Belingwe greenstone belt, Zimbabwe, *Geology*, **15**, 1147–1150, 1987.
- Nisbet, E. G., M. J. Cheadle, N. T. Arndt, and M. J. Bickle, Constraining the potential temperature of the Archean mantle: A review of the evidence from komatiites, *Lithos*, **30**, 291–307, 1993.
- Presnall, D. C., Alumina content of enstatite as a geobarometer for plagioclase and spinel lherzolites, *Am. Mineral.*, **61**, 582–588, 1976.
- Presnall, D. C., An algebraic method for determining equilibrium crystallization and fusion paths in multicomponent systems, *Am. Mineral.*, **71**, 1061–1070, 1986.
- Presnall, D. C., and J. D. Hoover, High pressure phase equilibrium constraints on the origin of mid-ocean ridge basalts, in *Magmatic Processes: Physicochemical Principles*, edited by B. O. Mysen, pp. 75–88, *Spec. Publ. Geochem. Soc.*, **1**, 1987.
- Presnall, D. C., N. L. Brenner, and T. H. O'Donnell, Drift of Pt/Pt10Rh and W3Re/W25Re thermocouples in single stage piston-cylinder apparatus, *Am. Mineral.*, **58**, 771–777, 1973.
- Presnall, D. C., S. A. Dixon, J. R. Dixon, T. H. O'Donnell, N. L. Brenner, R. L. Schrock, and D. W. Dycus, Liquidus phase relations on the join diopside-forsterite-anorthite from 1 atm to 20 kbar: Their bearing on the generation and crystallization of basaltic magma, *Contrib. Mineral. Petrol.*, **66**, 203–220, 1978.
- Presnall, D. C., J. R. Dixon, T. H. O'Donnell, and S. A. Dixon, Generation of mid-ocean ridge tholeiites, *J. Petrol.*, **20**, 3–35, 1979.
- Renner, R., E. G. Nisbet, M. J. Cheadle, N. T. Arndt, M. J. Bickle, and W. E. Cameron, Komatiite flows from the Reliance Formation, Belingwe Belt, Zimbabwe, I, Petrography and mineralogy, *J. Petrol.*, **35**, 361–400, 1994.
- Salter, V. J. M., and S. R. Hart, The hafnium paradox and the role of garnet in the source of mid-ocean-ridge basalts, *Nature*, **342**, 420–422, 1989.
- Schreinemakers, F. A. H., In-, mono-, and di-variant equilibria, I, *K. Ned. Akad. Wet. Proc. Sect. Sci.*, **18**, 116–126, 1915a.
- Schreinemakers, F. A. H., In-, mono-, and di-variant equilibria, II, *K. Ned. Akad. Wet. Proc. Sect. Sci.*, **18**, 531–542, 1915b.
- Schreinemakers, F. A. H., In-, mono-, and di-variant equilibria, III, *K. Ned. Akad. Wet. Proc. Sect. Sci.*, **18**, 820–828, 1915c.
- Sen, G., and D. C. Presnall, Liquidus phase relationships on the join anorthite-forsterite-quartz at 10 kbar with applications to basalt petrogenesis, *Contrib. Mineral. Petrol.*, **85**, 404–408, 1984.
- Shi, P., and G. Libourel, The effects of FeO on the system CMAS at low pressure and implications for basalt crystallization processes, *Contrib. Mineral. Petrol.*, **108**, 129–145, 1991.
- Stolper, E., D. Walker, B. H. Hager, and J. F. Hays, Melt segregation from partially molten source regions: the importance of melt density and source region size, *J. Geophys. Res.*, **86**, 6261–6271, 1981.
- Trull, T., S. Nadeau, F. Pineau, M. Polvé, and M. Javoy, C-He systematics in hotspot xenoliths: Implications for mantle carbon contents and carbon recycling, *Earth Planet. Sci. Lett.*, **118**, 43–64, 1993.
- Walter, M. J., Melting reactions of fertile garnet peridotite, *Eos Trans. AGU*, **76**(16), S297, 1995.
- Walter, M. J., and D. C. Presnall, Melting behavior of simplified lherzolite in the system CaO-MgO-Al<sub>2</sub>O<sub>3</sub>-SiO<sub>2</sub>-Na<sub>2</sub>O from 7 to 35 kbar, *J. Petrol.*, **35**, 329–359, 1994.
- Walter, M. J., T. W. Sisson, and D. C. Presnall, A mass proportion method for calculating melting reactions and application to melting of model upper mantle lherzolite, *Earth Planet. Sci. Lett.*, **135**, 77–90, 1995.
- Weng, Y.-H., and D. C. Presnall, Constraints on the depth of origin of komatiites based on melting relations in the system CaO-MgO-Al<sub>2</sub>O<sub>3</sub>-SiO<sub>2</sub> at 5 GPa, *Eos Trans. AGU*, **76**(46), F696, 1995.
- Zhang, J., and C. Herzberg, Melting experiments on anhydrous peridotite KLB-1 from 5.0 to 22.5 GPa, *J. Geophys. Res.*, **99**, 17,729–17,742, 1994.

G. H. Gudfinnsson, CETSEI, Department of Geology, University of Bristol, Bristol BS8 1RJ, England. (e-mail: g.h.gudfinnsson@bristol.ac.uk)  
D. C. Presnall, Magmology Laboratory, Department of Geosciences, University of Texas at Dallas, Richardson, TX 75083.

(Received January 31, 1996; revised July 3, 1996; accepted July 11, 1996.)